C. R. Palevol 10 (2011) 21–33

Contents lists available at ScienceDirect

Comptes Rendus Palevol

www.sciencedirect.com

Human palaeontology and prehistory

A late Middle Pleistocene hominid: Biache-Saint-Vaast 2, North France

Un hominidé de la fin du Pléistocène moyen : Biache-Saint-Vaast 2, Nord de la France

Gaspard Guipert[a,*], Marie-Antoinette de Lumley[b], Alain Tuffreau[c], Bertrand Mafart[a,b]

[a] *Antenne de l'institut de paléontologie humaine, europôle méditerranéen de l'Arbois, bâtiment Villemin, BP 80, 13145 Aix-en-Provence cedex, France*
[b] *Département de préhistoire, Muséum national d'histoire naturelle, UMR CNRS 5198, institut de paléontologie humaine, 1, rue René-Panhard, 75013 Paris, France*
[c] *Laboratoire de préhistoire et quaternaire, université des sciences et technologies de Lille, 59650 Villeneuve-d'Ascq, France*

ARTICLE INFO

Article history:
Received 22 September 2008
Accepted after revision 21 October 2010
Available online 30 November 2010

Presented by Yves Coppens

Keywords:
Biache-Saint-Vaast 1
Biache-Saint-Vaast 2
Homo heidelbergensis
Homo neanderthalensis
North France

ABSTRACT

Among the Middle Pleistocene human remains discovered in Biache-Saint-Vaast (Pas-de-Calais, France), three cranial fragments were attributed to the same individual: Biache-Saint-Vaast 2 (BSV2). Three-dimensional virtual imaging methods have been used to assemble the various bones and to study the endocranial cavities. The fact that these remains showed most of the classical Neanderthal characteristics as well as several plesiomorphic characteristics suggests the existence of a phyletic relationship with the early European Neanderthals.

Mots clés :
Biache-Saint-Vaast 1
Biache-Saint-Vaast 2
Homo heidelbergensis
Homo neanderthalensis
Nord de la France

RÉSUMÉ

Parmi les restes humains découverts à Biache-Saint-Vaast (département du Pas-de-Calais, France) et datés du Pléistocène moyen tardif, trois fragments crâniens ont pu être attribués à un même individu : Biache-Saint-Vaast 2 (BSV2). L'imagerie numérique tridimensionnelle a été utilisée pour articuler et étudier virtuellement les différents ossements. L'observation, sur ces restes, d'une majorité de caractères observés chez les Néandertaliens classiques associés à plusieurs caractères plésiomorphes est en faveur d'une appartenance phylétique aux premiers Néandertaliens d'Europe.

1. Presentation of the Biache-Saint-Vaast fossils

1.1. Location of the Biache-Saint-Vaast site

Biache-Saint-Vaast (Pas-de-Calais Department, France) is located between the towns of Arras and Douai in a valley on the left bank of the Scarpe River. The site (50°18′N, 02°56′E), which is located at mid-height in this valley at an altitude ranging between 44 and 56 meters, is oriented south/southeast (Sommé et al., 1988). This open site was discovered on 24 April 1976 during excavation work at the Usinor iron foundry. Rescue excavations directed by A. Tuffreau, which continued up to 1982 (Tuffreau, 1988a; Tuffreau et al., 1982), led to the discovery of several human remains among the many faunal remains present at this site.

* Corresponding author.
E-mail address: gaspard.guipert@gmail.com (G. Guipert).

1631-0683/$ – see front matter
doi:10.1016/j.crpv.2010.10.006

1.2. Datation

All the human remains originated from layer IIa (Tuffreau, 1988b), where the average age is 175 ky ± 13 ky (TL) (Huxtable and Aikten, 1988) and 253 + 53/– 37 ky (ESR) (corresponding to marine isotopic stages 6 and 7) (Yokoyama, 1989). They were associated with lithics and faunal remains. The continental flora and fauna detected, which were of the "moderate" type, suggest that this level and the human fossils it contains date back to the beginning of stage 7 (7a), and that their age is more nearer to 200,000 than 150,000 years BP (Sommé et al., 1988).

1.3. Human remains

Two fragmented human skulls were excavated at two places in layer IIa. Fragments of the parietal and temporal bones, an almost complete occipital bone, a portion of the *maxilla* and 11 teeth were discovered in situ in May 1976 (Vandermeersch, 1978). These remains (which were denoted Biache-Saint-Vaast 1 or BSV1) were initially attributed to a young female whose age-at-death ranged between adolescence and the early adulthood. According to Rougier (2003), however, the sex of BSV1 cannot be determined. A female attribution has been suggested in view of the fact that some of the traits of this skull are not very highly developed (Rougier, 2003). These traits include a whole set of Neanderthal anatomical characteristics: a small mastoid process, a rounded cranial contour in the coronal plane, and an occipital chignon. A phyletic position between late *Homo heidelbergensis* and the first *Homo neanderthalensis* has been proposed for this fossil (Dean et al., 1998; Rougier, 2003; Vandermeersch, 1978, 1982).

The other human bone fragments were identified on 8 November 1986 by P. Auguste during a study on the faunal bones. They originated from the same archeostratigraphic level as the other human remains and included a frontonasal fragment and fragments of the left parietal bone, the left temporal bone and the sphenoid and occipital bones. An anatomical connection was traced between the temporal bone, the greater wing of the left sphenoid bone, and the left parietal bone, which suggested that they belonged to the same individual (Biache-Saint-Vaast 2 or BSV2). The frontonasal and occipital fragments were also attributed to the same individual because their dimensions were compatible and because they were located in topographic proximity at the site.

The aims of the study on the BSV2 fossil were:

- to analyse its anatomical characteristics;
- to perform virtual reconstruction of BSV2;
- to discuss its phyletic position.

2. Preservation of the BSV 2 human remains

2.1. Frontonasal fragment

The frontal bone was damaged *post mortem* and is incomplete. The following parts of the frontal were found: most of the supraorbital torus, the base of the frontal squama, and the zygomatic process (Fig. 1). The metopic suture is not visible. Part of the coronal margin (9 mm) is preserved under the left stephanion. Synostosed fragments of the two nasal bones (maximum length of the right one: 5 mm) are preserved.

The frontal bone shows multiple disoriented fractures including three major ones. A posterior fracture extends transversely from the right frontotemporal landmark to the left third of the squama, from where it is prolonged obliquely towards the left coronal suture. A second fracture (D, Fig. 1) extends antero-posteriorly from the right third of the squama to the right supraorbital torus. A portion of the right supraorbital torus between the supraorbital notch and the glabellar area is missing from fracture D. A third fracture (G, Fig. 1) extends obliquely from the left external third of the squama to the left third of the left supraorbital torus.

Few gaps are present on the outer table of the squama.

2.2. Left parietal bone

This bone, of which only 6 fragments still exist (Fig. 2) corresponds to the lower half of the left parietal bone. The outer table includes some gaps. The coronal suture is no longer present. The most anterior point is located in the region of the sphenion. The upper fracture crosses almost the entire lower half of the bone, below the temporal lines. The inferior and superior temporal lines are conserved posteriorly. The posterior and lower limits of the bone are the lambdoidal and squamous sutures, both of which are incomplete.

2.3. Left temporal bone

The left temporal bone consists of 6 fragments (Fig. 2). It is the best preserved of all the BSV2 bones found. The upper part of the squama is fractured. This fracture is fairly curvilinear. The suprameatal crest is damaged. Part of the zygomatic process and the articular eminence are both preserved. The tympanic plate is complete. The external auditory meatus is intact. The posterior portion of the articular fossa is present. The mastoid notch is intact. The base of the styloid process is broken. The tegmen tympani is preserved.

The semicircular canals and the cochlea are preserved. The bony labyrinth was studied using 3-D imaging methods, and the results obtained will be presented below.

The endocranial surface was eroded *post mortem*. The groove of the occipital artery has been fractured distally with respect to the level of the juxtamastoidian eminence.

2.4. Sphenoid bone

Only 2 fragments of the temporal side of the left greater wing of the sphenoid bone are still present (Fig. 2).

2.5. Occipital bone

The 3 remaining fragments correspond to the basilar part of the occipital bone and the 2 condyles (Fig. 3). The right condyle is incomplete, whereas the left one is intact. The sphenoid-occipital suture is fused. Only the anterior part of the completely fused intra-occipital synchondrosis

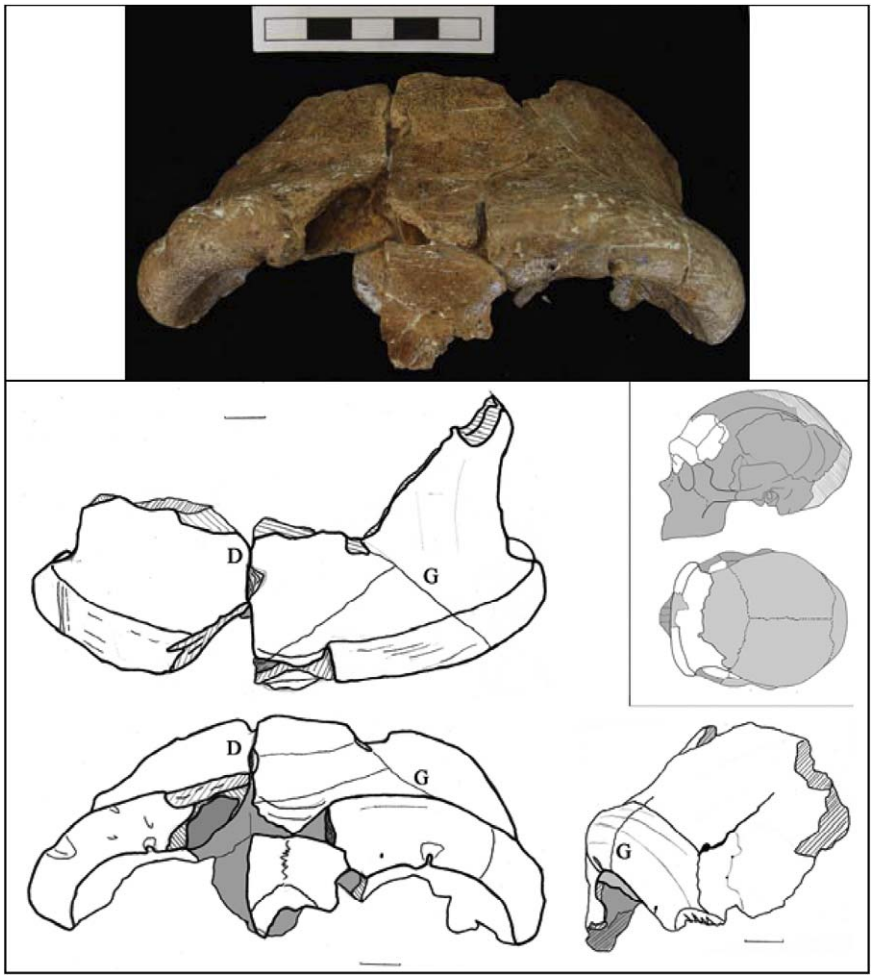

Fig. 1. Frontal bone of the Biache-Saint-Vaast 2 skull. Scale bar is 1 cm.
Fig. 1. Os frontal de Biache-Saint-Vaast 2. Barre d'échelle de 1 cm.

is still present. The proximal part of the left basilar region of the occipital bone is missing. Only the posterior part of the basilar gutter is still present. Laterally, the gutter of the lower petrous sinus is better preserved on the right side. The jugular tubercles covering the anterior condylar apertures are well preserved on both sides. The left jugular notch is well preserved. Laterally, the bone ends at the base of the occipital condyle.

3. Paleoanthropological study

3.1. Sex and age

It is difficult to estimate the age of this individual in the absence of teeth and long bones. The fractured frontal bone makes it possible to observe the presence of the frontal sinuses, but according to Trinkaus (1973), these are not reliable indicators to the attainment of adulthood However, the spheno-occipital synchondrosis was found to be fused, like the intra-occipital synchondrosis, which makes it possible to say that the BSV2 individual was an adult (Coqueugniot and Le Minor, 2002; Paturet, 1951; Scheuer and Black, 2000, 2004). This is compatible with the dimensions and the general robustness of the remaining fragments of this skull.

The Biache-Saint-Vaast 2 cranial fossils both have a fairly robust morphology, with a marked frontal torus and a thick parietal bone. Based on comparisons between the 2 human fossil remains originating from the Biache-Saint-Vaast site, BSV1 and BSV2, the parietal bone of BSV2 shows a fairly marked thickening between the superior and inferior temporal lines, and the mastoid process is more highly developed than in BSV1. These differences in the robustness of these two individuals may be sex-related differences: the BSV2 individual may have been a male and the BSV1 individual may have been a female. However we cannot rule out the possibility that these were simply inter-individual differences; whereas the possibility that the difference in size was an age-related difference can probably be ruled out: based on BSV1 age at death (Rougier, 2003) and BSV2, only slight differences in the posterior cranial growth can be expected to exist between BSV1 and BSV2, which is in line with the conclusions reached in the above comparisons.

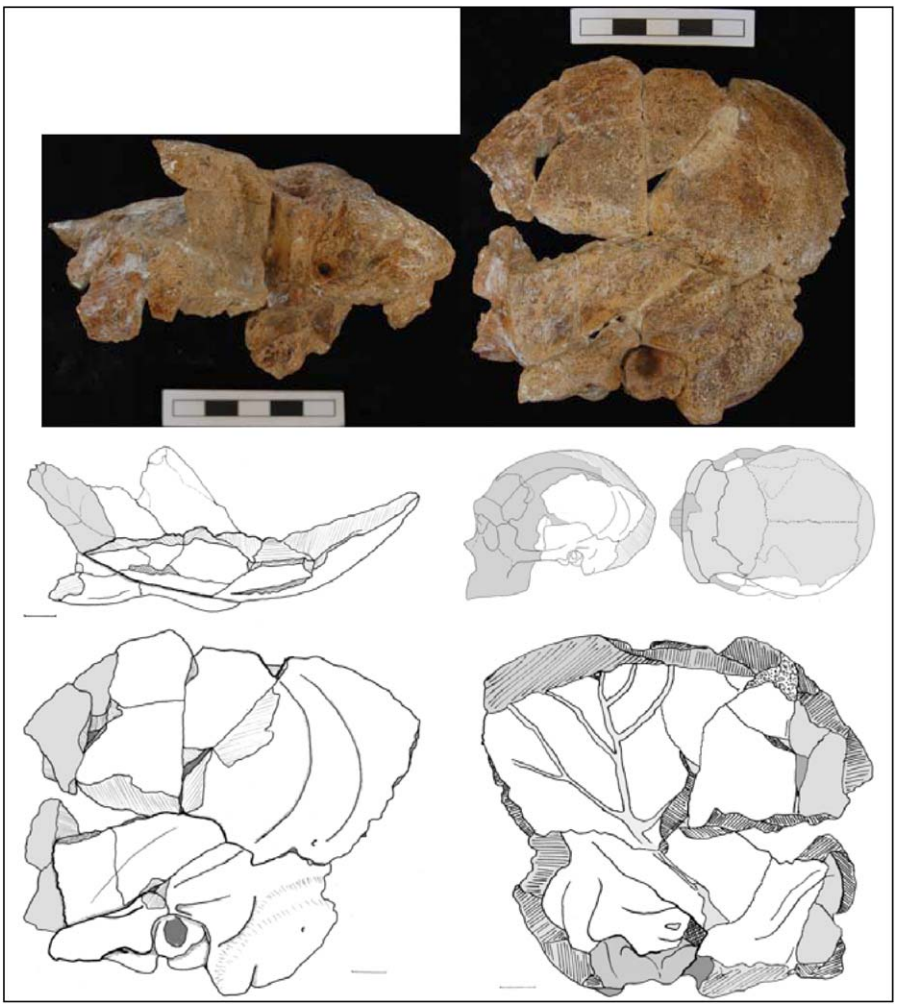

Fig. 2. Left parietal-temporal-sphenoid bones of Biache-Saint-Vaast 2. Scale bar is 1 cm.
Fig. 2. Os pariétal, temporal, sphénoïde de Biache-Saint-Vaast 2. Barre d'échelle de 1 cm.

3.2. Anatomical description

3.2.1. Frontal bone

Only the lower part of the frontal bone can be studied. The circumference of the orbits is round. One right supraorbital notch, one right supraorbital foramen and one left notch are present. The supranasal region is rough. The surface of the orbital arch and that of the right zygomatic process of the frontal bone are vermiculated. The supraorbital torus is of type III in Cunningham's scheme of classification (Cunningham, 1908). The thickness of the supraorbital torus is roughly similar on both sides. There is a marked asymmetry, however, in the lateral third of the supraorbital torus, since a bone depression is present on the right side. The pronounced left and right supratoral sulci are separated by the glabellar region. BSV2 possesses a relatively shallow supratoral sulcus above the glabella. The thickness of the frontal squama decreases along an anteroposterior gradient. No sagittal torus is visible. The post-orbital constriction is particularly marked. Laterally, a longitudinal depression separates the frontal squama from the left temporal line. This temporal line is smooth and rather curved.

The depth of the left temporal surface with respect to the temporal line is more than 10 mm. This feature cannot be measured on the right side.

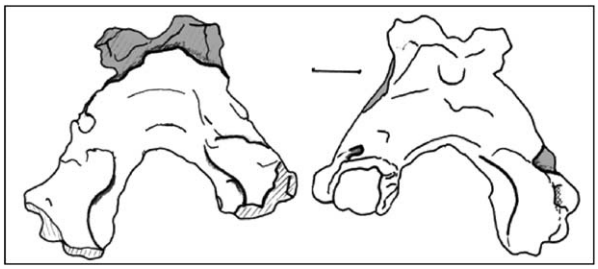

Fig. 3. Occipital bone of Biache-Saint-Vaast 2. Superior view on the left and inferior view on the right. Scale bar is 1 cm.
Fig. 3. Os occipital de Biache-Saint-Vaast 2. Vue supérieure à gauche, vue inférieure à droite. Barre d'échelle de 1 cm.

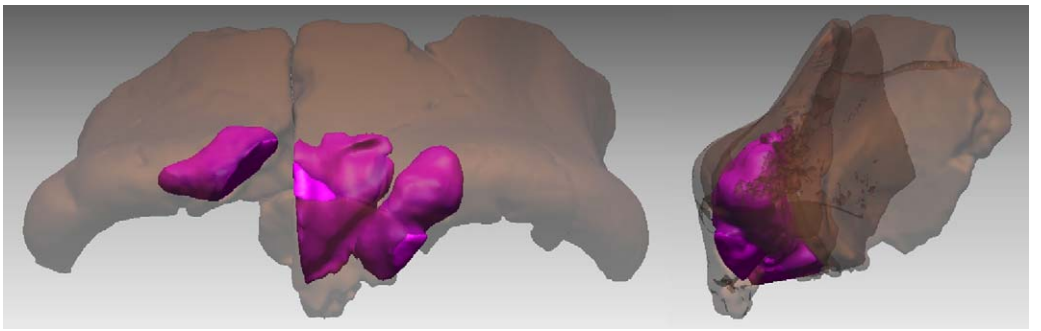

Fig. 4. Frontal sinuses of Biache-Saint-Vaast 2 after virtual reconstruction.
Fig. 4. Sinus frontaux de Biache-Saint-Vaast 2 après reconstruction virtuelle.

The frontal sinuses are well developed (Fig. 4) and asymmetric. The left one is smaller and separated from the right one by a septum oriented to the left. The left sinus does not reach the left supraorbital notch. The right sinus reaches the middle of the right supraorbital torus. The superior part of the right sinus ends just before the supratoralis sulcus.

In the endocranial view, the frontal crest was found to measure 10 mm in height and more than 40 mm in length. Its lower base is not preserved, as observed in the case of the foramen cecum. The crest is frayed and curvilinear at the bottom, while the upper part widens and deviates toward the right. The sagittal sulcus and the orbital plate are no longer present. The cerebral convolutions are barely visible.

3.2.2. Parietal bone

The parietal bone is thick (11 mm at the top of the lambdoidal suture). In the posterior part, an osseous thickening fills the space between the inferior and superior temporal lines. Posteriorly, a change in the parietal bone curve was observed just under the superior fracture. This may correspond to a similar prelambdatic depression to that observed within the occipital chignon.

In the endocranial view, the meningeal impressions are very strongly marked. The groove in the bregmatic branch of the middle meningeal artery is not visible because its contour merges with the anterior fractures of the parietal bone. The lambdatic branch of the middle meningeal artery reaches the posterior third of the parietal bone. Its groove is strongly marked, 1.5 mm wide, and gives rise to at least 2 collaterals. The well preserved distal groove in the lambdatic branch approaches the lambdoidal suture: the first collateral turns off towards the vertex before reaching this suture and then merges with the fracture. The end of the obelian lambdatic branch is trifurcated.

3.2.3. Temporal and sphenoid bones

The supramastoid crest is strongly marked and smooth. The suprameatal crest cannot be described because of a gap. The mastoid crest is also marked and along with the supramastoid crest, it delimits a supramastoid sulcus. No anterior mastoid tubercles (Hublin, 1978) seem to be present behind the external auditory meatus. The mastoid process is small and slightly rounded. It can be seen in the lateral view to be antero-inferiorly directed. In the posterior view, this process is directed towards the interior of the cranium.

The external auditory meatus is elliptical, and its main axis is oriented from superior to inferior. The thickness of the tympanic plate decreases from the back to the front. No clearly distinguishable parts could be seen in the tympanic plate. The tympanic part is orientated coronally. A *spina suprameatum* surmounts the external auditory meatus and delimits a suprameatal triangle. The external auditory meatus is in the axis of the zygomatic process.

Anteriorly, the entoglenoid process is prominent. The articular eminence is also proportionally small. The notch corresponding to the articular fossa is not very deep. This articular fossa looks rather narrow.

The digastric groove, the base of the styloid process and the stylomastoid foramen are not aligned because the styloid process is more medially placed.

The juxtamastoid eminence has a semi-circular shape from the top of the eminence (posteriorly with respect to the mastoid foramen) to the antero-inferior end. This crest does not show an occipital part, but the juxtamastoid eminence reaches the occipito-mastoid suture, which it follows without crossing it before passing it by. The juxtamastoid eminence, which was not found to be divided by the occipital groove, is more highly developed than the mastoid process.

The mastoid notch does not join the stylomastoid foramen. The mastoid notch is broad and looks open anteriorly, but includes a small medial bone elevation. The walls of the mastoid notch are very steep, which contributes to its triangular contour, forming a V-shaped pattern.

The preserved portion of the sphenoid bone is very small. No anatomical observations could be carried out on this cranial component, but it does not seem to be very thick.

3.2.4. Occipital bone

Between the 2 basilar surfaces, the pharyngeal tubercle lying opposite the pharyngeal fossette is only slightly marked.

4. Virtual reconstruction and morphometric study

Virtual imaging methods were used to check the position of the fragmented remains that were reassembled

manually after their discovery, and to propose a virtual assembly of the various cranial fragments on which to base our comparisons between BSV2 and other cranial fossils from the Middle and Late Pleistocene periods. Although we could have completely cleaned the fragments and reconstructed the skull manually, we decided to use medical imaging methods in order to protect the fossil from further damage.

4.1. Virtual imaging methods

Virtual reconstruction was performed by isolating the fragments and reassembling the pieces using CT scans and 3-D image processing methods. The fragments were CT scanned with a General Electric Light Speed scanner at the *Centre hospitalier national d'ophtalmologie des Quinze-Vingts* Radiology Unit, Paris (settings: 120 kV, 495 mAs, slice thickness 0.625 mm, field of view 250 mm, pixel size 0.32 mm, matrix 512 × 512 pixels, Dicom format). 3-D reconstruction was carried out by post-processing the CT data using the Mimics 9.0 software program (Materialise©).

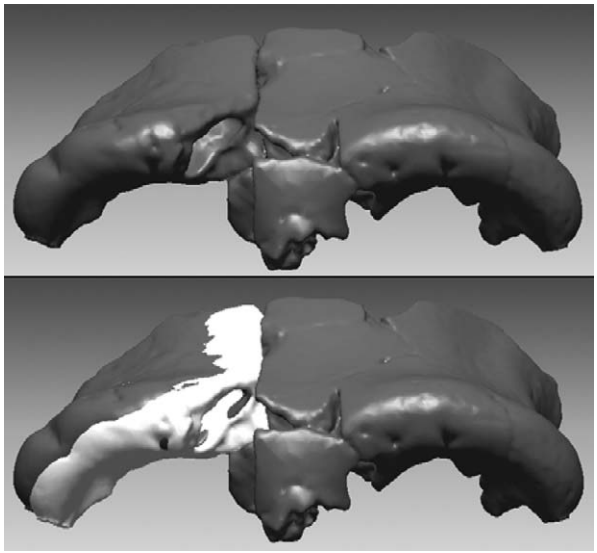

Fig. 5. Frontal bone after virtual reconstruction and superimposition (white: before reconstruction).
Fig. 5. Os frontal après reconstruction et superposition (blanc : avant reconstruction).

4.2. Virtual repositioning of the frontal and sphenoid fragments

When first discovered, the right and left frontal fragments were stuck together in the wrong position, resulting in an unnatural degree of asymmetry. The fragments of the left greater wing of the sphenoid bone were also incorrectly assembled. In order to prevent the risk of damaging the fossils when intervening directly on the fragments, virtual repositioning methods were used. The frontal fragments were assembled in line on the right plane of fracture (D) (Fig. 5). This required finer positioning of the external edge of the right fragment. This newly positioned frontal bone is now more divergent distally. The maximum width of the frontal torus has increased, ranging from 121 to 127.8 mm.

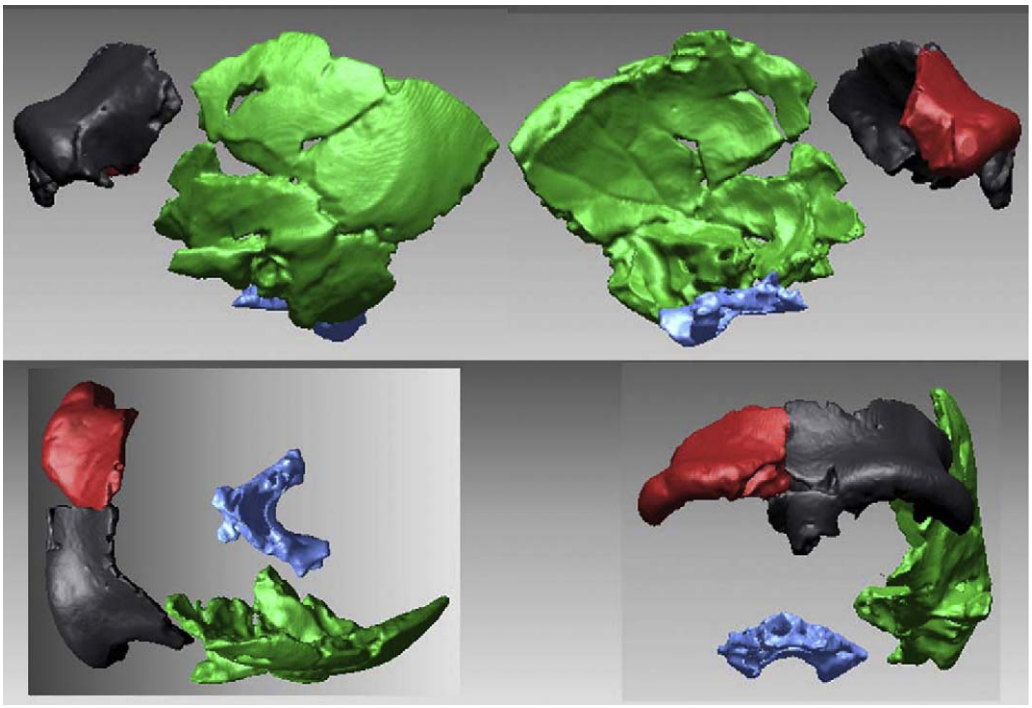

Fig. 6. 3-D positioning of the fragments of Biache-Saint-Vaast 2.
Fig. 6. Positionnement spatial en 3-D de Biache-Saint-Vaast 2.

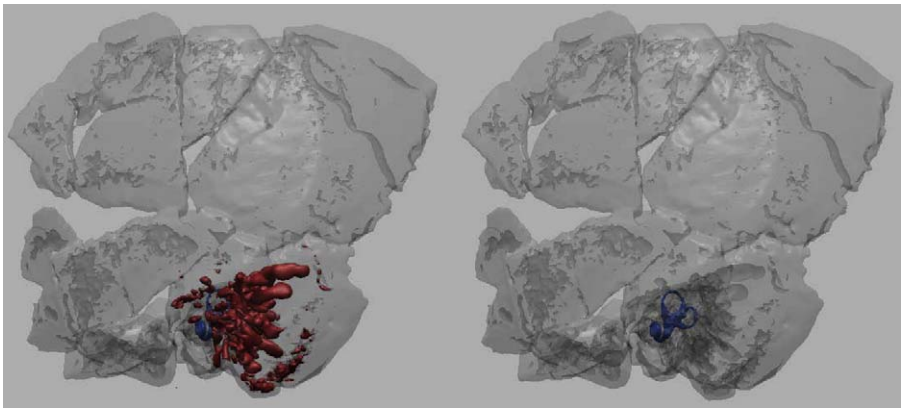

Fig. 7. Pneumatisation of the petromastoid area and bony labyrinths of BSV2.
Fig. 7. Pneumatisation de la région pétromastoïdienne et labyrinthe de Biache-Saint-Vaast 2.

The fragments of the left greater wing of the sphenoid bone were dissociated in the same way.

4.3. Virtual repositioning of the cranial fragments

The various bone fragments were then repositioned in relation to each other (Guipert et al., 2007). The sagittal plane was defined using the frontal bone and the basilar part of the occipital bone. The parietal bone was positioned in relation to the frontal bone at the edges of the fracture, corresponding to the area of the coronal suture, and at the curve of the temporal surface of the frontal bone. However, a gap still exists between the 2 fragments. The basilar fragment was used to direct and position the base of the parietal-temporal-sphenoid of BSV2 (Fig. 6).

The accuracy of the virtual positioning was tested using a chimera. The posterior part was assembled by mirroring the BSV2 parietal, temporal, and sphenoid bones and adding the upper part of the BSV1 parietal bones and the BSV1 occipital bone. Because of the deformations undergone by BSV1, we mirrored the right side. BSV1 was used for this purpose because the two skulls are of a similar size and shape. The frontal squama was reconstructed by mirroring the right side of Krapina 3, another anatomically similar skull. This enabled us to simulate the orbital rim and to model the Frankfurt plane. The chimera thus obtained served to check the accuracy of the positioning of the BSV2 remains.

4.4. Three-dimensional exploration of the temporal bone

The petromastoid region of the temporal bone of BSV2 is highly pneumatised (Fig. 7). The cochlea is well preserved (Fig. 8). 3-D modelling was performed in order to determine the shape characteristics of the semicircular canals. The upper origin of the arch of the posterior semicircular canal is horizontal and projected to below the upper half of the arch of the anterior semicircular canal. The lateral semicircular canal projected onto the upper half of the posterior canal. In the upper view, the lateral semicircular canal is not separated from the posterior semicircular canal.

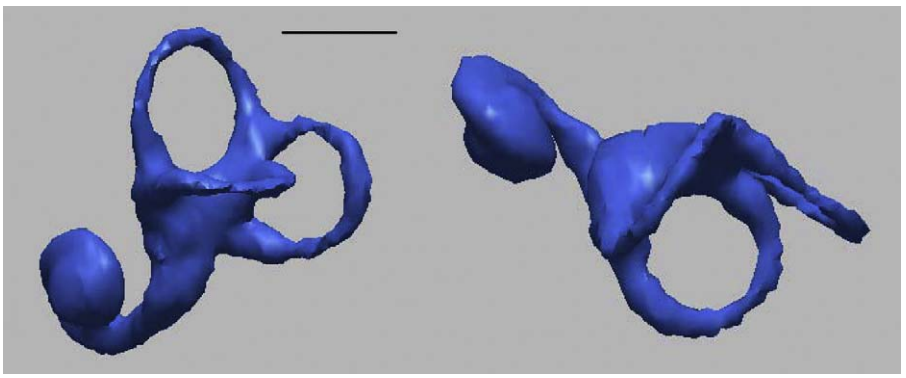

Fig. 8. Lateral and superior aspects of the left bony labyrinths of BSV2 reconstructed from sagittal CT scans. The lateral view is aligned with the plane of the lateral semicircular canal. Scale bar is 5 mm.
Fig. 8. Aspect latéral et supérieur du labyrinthe de BSV2, reconstruit à partir de balayages sagittaux par rayonnement X. La vue latérale est alignée sur le plan du canal semicirculaire latéral. Barre d'échelle de 5 mm.

Table 1
Measurements of frontal, parietal, temporal and occipital bones in mm.
Tableau 1
Mesures des os frontaux, pariétaux, temporaux et occipitaux en mm.

	M9	A	M43	M27(1)	M30(1)	M30(1)/M27 × 100	B	C	B/C	D	M16
BSV2	**104.4**	**128.7**	**127.6**	**(87.5)**	**(81.6)**	**(93.2)**	**80.5**	**61**	**75.8**	**40.1**	**29.6**
Sima de los Huesos 5[a]	105.7	(129.3)	129.3	91.4	87.1	95.3	77.4	56.8	73.4	48	25.7
Kabwe	101	139.5	133.6	105	98.3	93.6	86.8	74.4	85.7	35.7	(31.5)
Petralona	110	133	131	111	100.6	90.6	96	65	67.7	–	31.1
Saccopastore I[b]	119	–	114	97	91	93.8	–	61	–	–	28
Gibraltar I[c]	100	–	118	–	–	–	–	–	–	–	–
La Ferrassie I[c]	109	119.9	121	104.5	99.2	94.9	85[f]	72[f]	84.7	35.4	34
La Chapelle-aux-Saints[c]	109	123.5	123.5	107	99.6	93.1	82[f]	58[f]	70.7	35.6	30
La Quina H5[c]	100.2	111.7	112.5	–	–	–	80[f]	58[f]	72.5	36.5	–
La Quina H27[d]	–	–	–	–	–	–	–	56	–	–	–
Monte Circeo 1	109	(120)	(120)	103.4	95	91.9	84	61	72.6	24.9	-
Neandertal 1	108	120.5	120	–	(110.9)	–	–	–	–	–	–
Krapina 3 (right)[e]	103	120.7	120.7	99.1	92.8	93.6	81.7	58[c]	71	34.2	–
Amud 1	113.5	125.6	122.7	106.5	100.6	94.5	86.2	67	77.7	45.6	–
Mean *H. neanderthalensis*	107.9	120.3	119.2	102.9	98.4	93.6	83.2	61.4	74.9	35.4	30.7
Skhul V	103.5	123.8	123.8	96	92.3	96.1	87.3	67.8	77.6	40.1	29.5
Qafzeh 9	103	111.7	111.7	99	95.8	97	81	66.3	81.5	38 (right)	–

M9, M43, M27(1), M30(1) are from Martin and Saller (1957). M9: Minimum frontal breadth; M43: Maximum anterior frontal breadth; M27(1): Left parietal-temporal arc; M30(1): Left parietal-temporal chord; A: Maximum torus width; B: Length of the left temporal bone; C: Length of the squama of the left temporal bone; D: Projection of the left mastoid process from the parietal notch. Measurements obtained on casts are underlined.

[a] Arsuaga et al., 1997.
[b] Condemi, 1992.
[c] Heim, 1976.
[d] Vallois, 1969.
[e] Smith, 1976.
[f] Mean value between left and right sides.

4.5. Morphometric and morphological study

4.5.1. Frontal bone

The interorbital breadth is 23 mm. The thickness of the squamous part of the frontal bone ranges between 6 and 7 mm. The minimum frontal breadth (M9 according to Martin and Saller, 1957; Table 1) after reconstruction is 104.4 mm. The maximum width of the frontal torus is 128.7 mm, and the breadth M43 is 127.6 mm. The breadth of the frontal sinus (Tillier, 1977) is 64.2 mm, corresponding

Table 2
Frontal sinus dimensions in mm.
Tableau 2
Dimension des sinus frontaux en mm.

	1	2	3	4	5	6	7	8
BSV2	**30.0**	**17.0**	**2.3**	**64.2**	**42.0**	**22.0**	**21.6**	**18.7**
Kabwe (Broken Hill)	51.4	23.0	5-6	80.5	40	40.5	38.5	23.5
Steinheim	17.5	15.0	–	60	–	–	–	–
Ehrinsdorf III	42.0	18.0	–	80	–	–	–	–
Saccopastore I	29.0	12.0	–	65.0	–	–	–	–
Saccopastore II	30.0	16.0	–	–	–	–	–	–
Gibraltar I	–	–	–	52.6	20.6	29.0	10.7	13.5
La Ferrassie I	37.6	18-20	3.2	83.8	48.8	32.0	20.5	20.3
La Chapelle-aux-Saints	23.7	16-20	2.9	58.8	27.2	31.6	12.8	14.5
La Quina H5	33.5	15.6	2.7	66.0	31.6	29.2	–	–
Spy I	29.4	17.0	3.0	78.2	–	–	15.0	18.5
Spy II	16.7	16.0	2.3	64.5	–	–	–	–
Monte Circeo 1	23.6	16.3	4.0	73.1	29.8	39.8	17.5	21.5
Neandertal 1	30.0	20.0	3.5	65.0	30.0	35.0	11.0	14.6
Krapina 5	28.0	10.0	–	56.0	–	–	–	–
Krapina 3	33.0	12.0	–	71.0	35.0	36.0	20.7	15.1
Tabun I	24.2	10.4	3.1	52.1	22.6	24.5	5.9	13.0
Sala	29.0	18.0	–	52.0	27.0	25.0	–	–
Skhul V	23.0	15.1	–	–	–	–	–	–
Qafzeh 3	31.5	17.6	2.0	–	–	–	–	–
Qafzeh 6	21.5	15.4	2.9	61.0	26.5	31.9	12.3	16.2

Measurements from Tillier (1977).
1 : height of the frontal sinus ; 2 : anteroposterior size of the frontal sinus; 3: thickness of the glabellar wall; 4: breadth of the frontal sinus; 5: left sinus breadth; 6: right sinus breadth; 7: height of the left sinus above the orbital rim; 8: height of the right sinus above the orbital rim.

Table 3
Bony labyrinth measurements.
Tableau 3
Mesures des canaux semi-circulaires.

		ASC-R	PSC-R	LSC-R	ASC %R	PSC %R	LSC %R	ASCh/w	PSCh/w	LSCh/w
BSV2		**3.01**	**2.74**	**2.59**	**36.2**	**32.8**	**31**	**94.35**	**106.41**	**97.14**
Neanderthal lineage	Mean	2.99	2.81	2.57	35.76	33.52	30.7	93.45	99.90	91.56
	S.D.	0.2	0.21	0.17	1.24	1.42	1.05	4.97	9.94	7.08
	n	25	25	25	25	25	25	25	25	25
Middle Paleolithic modern humans	Mean	3.32	3.03	2.37	38.1	34.7	27.2	88.5	99.7	83.4
	S.D.	0.20	0.16	0.18	1.3	1.6	1.6	6.9	7.9	9.7
	n	11	11	11	11	11	11	11	11	11
European Upper Paleolithic	Mean	3.30	3.05	2.54	37.2	34.2	28.5	88.1	109.3	93.7
	S.D.	0.20	0.32	0.24	1.2	1.9	1.0	5.8	7.1	5.4
	n	7	7	7	7	7	7	6	6	6
Nazlet Khater		3.6	3.0	2.5	39.5	32.5	28	82	96	86
Extant Human	Mean	3.25	3.17	2.34	37.1	36.2	26.7	90.5	105	92.1
	S.D.	0.20	0.26	0.20	1.2	1.6	1.7	4.5	7.2	6.2
	n	134	134	134	134	134	134	134	134	134

Values from Bouchneb and Crevecoeur (2009).

to a sinus height of 30 mm and an anteroposterior size of 17 mm (Table 2). The thickness of the glabellar wall is 2.3 mm. The breadth of the left frontal sinus is 42 mm, and that of the right one is 22 mm. The height of the sinus above the orbital rim is 21.6 mm in the case of the left sinus, and 18.7 mm in that of the right one. The volume of the frontal sinus is about 9021 mm^3.

4.5.2. The parietal, temporal and sphenoid bones

The parietal-temporal arc M27(1) was found to measure 87.5 mm in length, with a chord M30(1) 81.6 mm in length. The parietal-temporal index of the curve therefore is calculated to be 93.2. The preserved portion of the lambdoidal suture measures 54.7 mm. The maximum width between the superior and inferior temporal lines is 16 mm. The thickness of the parietal bone ranges between 12 mm at the level of the thickening between the temporal lines, 10.4 mm at the level of the asterion, and 9.2 mm at the level of the parietal notch.

The total length of the temporal bone is 80.5 mm. The length of the squama is 61 mm. The height of the squama cannot be determined because of the poor state of conservation of the inferior part of the parietal bone. The thickness at the center of the squamous part of the temporal bone is 8.3 mm. The distance between the parietal notch and the antero-inferior extremity of the mastoid process (Martinez and Arsuaga, 1997) is 40.1 mm. The thickness of the tympanic plate at its central point is 6.2 mm. The length and width of the articular fossa (Condemi, 2001) are 20.1 and 19.9 mm, respectively.

The thickness of the zygomatic process varies relatively little. Four thicknesses were measured as described by Condemi (2001): in front of the external auditory meatus (13.5 mm), before the articular eminence (7.1 mm), at the maximum thickness of the articular eminence (9.6 mm), and anteriorly to the articular eminence (6.9 mm).

The pneumatised part of the petromastoid region occupies a volume of 2054 mm^3. Some of the pneumatic cells are relatively large, especially those located in the posterior and postero-inferior parts of the temporal bone. The dimensions of the semi-circular canals given in Table 3 were based on studies by Spoor and Zonneveld (1998) and Spoor et al. (1994, 2003). The anterior semicircular canal has a radius of curvature ($R = 0.5 \times$ [height + width]/2) of 3.01 mm (relative radii of the semicircular canals, 36.2 %), which is larger than that of the other 2 canals (Table 3). The shape indices (height/width $\times$ 100) range between 106.41 in the case of the posterior canal and 94.35 in that of the anterior canal.

No measurements can be obtained on the severely damaged sphenoid bone.

4.5.3. Occipital bone

The width of the foramen magnum (M16: 29 mm) was determined by mirroring the occipital fragment. The left occipital condyle is 19.9 mm long, 13.5 mm wide and 7.3 mm high.

4.5.4. Morphological study

Two profiles were drawn up in order to compare BSV2 with Middle and Late Pleistocene hominids originating from Europe and the Middle East: Arago 21, Sima de los Huesos 5, Petralona, La Chapelle-aux-Saints, Neanderthal, La Ferrassie 1, Monte Circeo 1, Amud 1, Krapina 3, and Biache-Saint-Vaast 1.

The chimera was used to position the BSV2 frontal bone with respect to the Frankfurt plane. The various skull profiles were aligned by superimposing the nasion (Fig. 9).

A coronal profile of the parietal and temporal bones was drawn up, using the parietal notch and the antero-inferior extremity of the mastoid process as landmarks (Fig. 10). Using the chimera, the BSV2 remains were aligned with the other skulls, based on the Frankfurt plane. The profiles were superimposed using the extremity of the mastoid process as a landmark. This plane was chosen because few other landmarks were available.

The sagittal profile of the preserved portions of the frontal bone of BSV2 is similar to that of Krapina 3. The profile of the glabellar area of BSV2 showed a weaker curvature than that of Arago 21, La Ferrassie 1, Neanderthal, and La Chapelle-aux-Saints, whereas the nasion of BSV2 was located anteriorly. The glabellar area of Sima de los Huesos 5 is higher than that of Biache-Saint-Vaast 2. The cranium

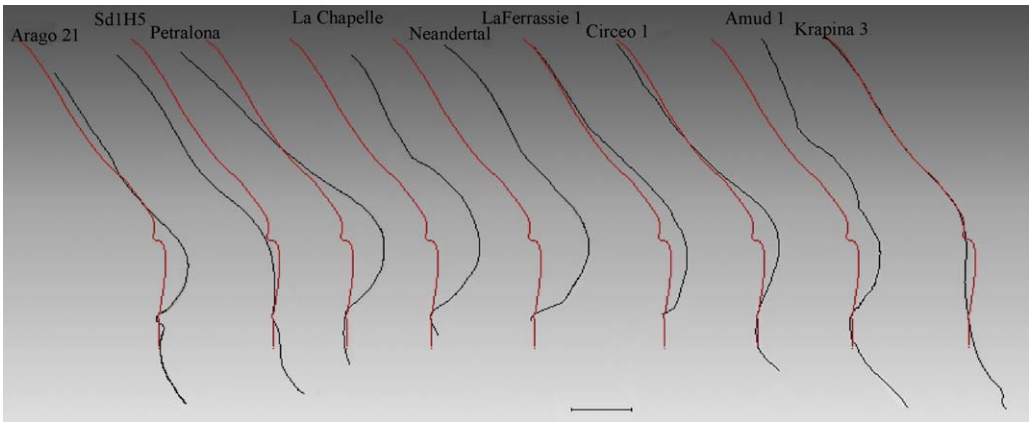

Fig. 9. Comparison between the sagittal frontal profile of BSV 2 (red) and those of other European hominid fossils. The profiles are aligned on the basis of the Frankfurt plane and the nasion. Scale bar is 1 cm.
Fig. 9. Comparaison des profils sagittaux frontaux de BSV2 (rouge) avec ceux d'autres hominidés fossiles d'Europe. Les profils sont alignés selon le plan de Francfort et le nasion. La barre d'échelle est de 1 cm.

of Petralona, which has a more curved glabellar area and a less raised frontal squama, differs the most from the other skulls compared.

The layout of the parietal-temporal profile of Biache-Saint-Vaast 2 is similar to that of Biache-Saint-Vaast 1. It was also found to be similar to that of Krapina 3 (after mirroring) up to the level of the temporal lines. The Amud 1 mastoid process is longer in this profile. The parietal bones of La Ferrassie 1, La Chapelle-aux-Saints, Monte Circeo 1, and La Quina H5 are more convex than that of BSV2; on the other hand, the parietal-temporal profile of Sima de los Huesos 5 is more vertical. Petralona yielded a very different profile, with a more oblique parietal bone.

5. Discussion of the phyletic position of BSV2

The human fossil remains known as Biache-Saint-Vaast 2 show a set of plesiomorphic and apomorphic characteristics known to exist in late *Homo heidelbergensis* in Europe and in the early and classical Neanderthals (Dean et al., 1998).

As far as the frontal bone is concerned, the supraorbital torus of BSV2, which is of type III in Cunningham's system of classification (1908), resembles that present in the last European *Homo heidelbergensis* (as well as that of Sima de los Huesos 5 and Bilzingsleben) and the Neanderthals (Spitery, 1984).

The minimum frontal breadth of BSV2 is smaller than the mean Neanderthal value (Table 1). However, it is larger than in Krapina 3 and La Quina H5. In *Homo heidelbergensis*, only Kabwe has a smaller M9 breadth than BSV2. On the other hand, the frontal torus of BSV2 is very broad. Only Sima de los Huesos 5, Kabwe and Petralona show higher M43 values and the absolute maximum breadth. This broad torus, associated with a low minimal breadth (M9), accentuates the post-orbital constriction. This constriction is more marked than that of the classical Neanderthals such as La Chapelle-aux-Saints or La Ferrassie 1.

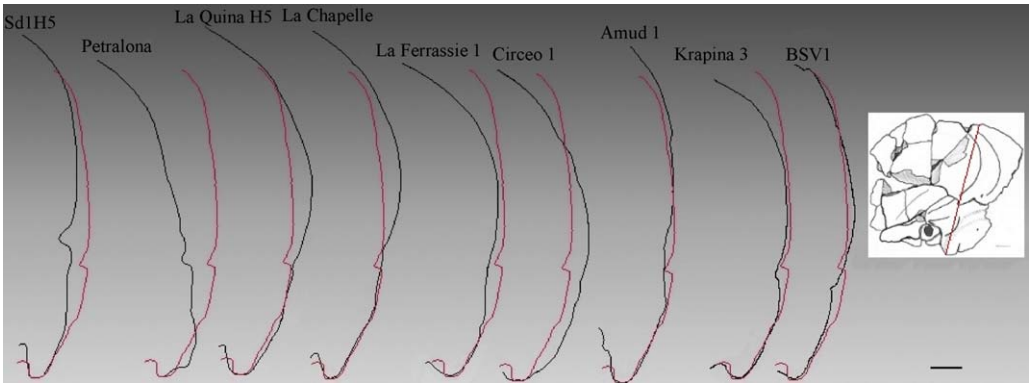

Fig. 10. Comparison between the parietal and temporal bone profile of BSV 2 (red) and those of other European hominid fossils. The profiles are aligned on the basis of the antero-inferior point of the mastoid process and the parietal notch. Scale bar is 1 cm.
Fig. 10. Comparaison des profils de l'os temporal et pariétal de BSV2 (rouge), avec ceux d'autres hominidés fossiles d'Europe. Les profils sont alignés suivant l'extrémité antéro-inférieure du processus mastoïdien et l'incisure pariétale. La barre d'échelle est de 1 cm.

The sagittal profile of the frontal bone is similar to that of Krapina 3. The frontal squama (Fig. 9) differs from that of all the *Homo heidelbergensis* skulls studied so far. Among these skulls, the Petralona skull shows the most different profile, including a less raised squama and a more prominent glabellar area. Arago 21 has a similar squama and a more anterior glabella. Sima de los Huesos 5 seems to have a similar squamal profile (parallel outlines) but is smaller than that of BSV2. The posterior enlargement of the preserved frontal squama is more progressive in Biache-Saint-Vaast 2, however, than in Sima de los Huesos 5. Except for Amud 1 (which yielded straighter outlines, the sagittal profile of the frontal squama of BSV2 is similar to those of the classic Neanderthals (parallel outlines) such as Monte Circeo 1, La Chapelle-aux-Saints, and La Ferrassie 1. However, these Neanderthals, unlike Krapina 3 (one of the early Neanderthals; Dean et al. (1998)), differ in terms of the anterior position of the glabella in relation to the nasion in the sagittal plane. The glabella of these fossils was projected. In these projections, the frontal torus of Krapina 3 is that resembling that of BSV2 most closely.

The frontal torus has a vermiculate surface resembling that present in Neanderthal adults, as described by Tappen (1978). However, the latter author specified that some modern individuals, such as some *Homo erectus,* also have surface characteristics of this kind.

The development of the frontal sinuses is comparable to that of the early and classic Neanderthals (Tillier, 1977; Vlček, 1967). The asymmetrical pattern of the frontal sinus corresponds anteriorly, laterally and superiorly to that of Monte Circeo 1 (Tillier, 1977): the left sinus is smaller than the right one, and the frontal sinus ends posteriorly before the supratoralis sulcus. The height, the anteroposterior thickness and the breadth of the frontal sinus are similar to the Neanderthal values measured by Tillier (1977) (Table 2).

The maximum width corresponds to the inferoposterior third of the theoretical biparietal vault. The parietal bone does not look as robust as the Arago 47 and Petralona fossils. The parietal bone was found to be larger than that of the other fossils compared here but the osseous thickening between the superior and inferior temporal lines does not occur in the classic Neanderthal crania. The osseous thickening is relatively marked in the BSV2 parietal bone, more than in BSV1 (Rougier, 2003). This may be a sex-related difference. However, this thickening is very slight in comparison with that described in Kabwe and Arago 47. It may also correspond to a plesiomorphic feature. A medial change in the parietal posterior curve was observed. This is probably a prelambdatic depression indicating the presence of an occipital chignon such as that of BSV1. This would correspond to the classic Neanderthals (Monte Circeo 1, La Chapelle-aux-Saints, Spy 2, and La Ferrassie 1). The parietal meningeal grooves observed in BSV2 are strongly marked, like those of the parietal impressions of Cova Negra and Lazaret (Lumley, 1973). It is proposed to carry out more exhaustive study of the endocranium of BSV2 in the future.

Comparisons between the parietal-temporal profiles showed the existence of similar contours in BSV1 and BSV2 (Fig. 10). The curve of the parietal-temporal bone in the coronal plane is more vertical than that of the classic Neanderthals such as La Chapelle-aux-Saints, La Ferrassie 1, i.e., fossils showing a more curved section, especially the parietal one. The curve of BSV2 differs from that of the *Homo heidelbergensis*. Petralona has a more slanting profile, showing maximum breadth at the level of the temporal bone. Sima de los Huesos 5 is more vertical. BSV2 resembles Amud 1 (classic Neanderthal). Krapina 3 (after mirroring) and La Ferrassie 1 have very similar temporal profiles, but the part of the parietal bone featuring on the temporal lines is more curved. La Quina H5 and La Chapelle-aux-Saints also showed identical temporal profiles to that of BSV2, along with a more curved parietal profile. However these curvatures are more convex than in Krapina 3 and La Ferrassie 1. Monte Circeo 1 has a more curved parietal and temporal profile. The various layouts obtained depended on the shape of the temporal bone (i.e., on the position of the parietal notch).

Anteroposteriorly, the temporal border of the parietal bone of BSV2 is short. Sima de los Huesos 5 has a relatively similar M30(1) chord. Among the Neanderthals, that of Saccopastore 1 is the most similar. The curvature of the temporal border is similar to the mean Neanderthal value, but the temporal borders of the latter fossils are longer. The maximum parietal breadth in BSV2 occurs at the level of the posterior third.

The temporal bone of BSV2 shows a set of characteristics, which are similar to those of the Neanderthals. The parietal notch has a similar layout (after inversion) to that of the right temporal bone of La Quina H27 (based on the layouts presented by Condemi, 1992). The squamous part corresponds to a quarter of the total length of the temporal bone (Table 1). It is small like those of the Neanderthals, except for La Ferrassie 1 and Amud 1. The temporal length is similar to that of the Neanderthals and differs from that of Kabwe and Petralona. The height of the temporal squama cannot be measured or assessed because of the poor state of conservation of the lower part of the parietal bone.

The mastoid process is small and rounded like that of Krapina 3, with a narrow digastric groove. In the posterior view, the mastoid process is directed medially, which contributes to giving it a rather rounded contour in the coronal plane, as observed with the Neanderthals, where it has been described as a full *en bombe* contour (Dean et al., 1998). The distance between the parietal notch and the antero-inferior extremity of the mastoid process (Martinez and Arsuaga, 1997) is greater than in the Neanderthals, but smaller than in Sima de los Huesos 5 (Table 1), possibly because the parietal notch occurs in a higher position.

As in the La Ferrassie 1, La Quina H5 and La Chapelle-aux-Saints skulls (Heim, 1976), the external auditory meatus is surmounted by a *spina suprameatum*. This external auditory meatus is in line with the zygomatic process, as occurs in the Neanderthals Monte Circeo 1, La Chapelle-aux-Saints, Spy 2 and La Ferrassie 1 (Condemi, 2001; Martinez and Arsuaga, 1997). The thickness of the zygomatic process is similar to that of La Chapelle-Aux-Saints, La Quina H5 and La Ferrassie 1, based on the values published by Condemi (2001), except for the portion anterior to the articular eminence, which is slightly less thick in BSV2.

No anterior mastoid tubercle of the kind described in the La Chapelle-aux-Saints skull (Hublin, 1978) was observed

on the preserved temporal bone. This structure may have been slightly more highly developed on the right temporal bone, as in the case of the La Ferrassie 1 and La Chapelle-aux-Saints fossils (Hublin, 1978). It can be concluded that this feature was probably little or not at all developed on the whole in BSV2. However, the mastoid crest is continuous and becomes quite broad and thick at its anterior end.

The digastric groove, the base of the styloid process and the stylomastoid foramen are not aligned, because the styloid process occurs more medially, as in Neanderthals (Elyaqtine, 1995). The juxtamastoid eminence is more highly developed than the mastoid process, which corresponds to an autapomorphous trait in the Neanderthals (Aiello and Dean, 1990; Condemi, 1988, 1992; Heim, 1976; Hublin, 1988a, 1988b; Santa Luca, 1978; Trinkaus, 1983, 1988).

In comparison with the articular fossae measured by Condemi (2001), the articular fossa of BSV2 is rather narrow, and it is much shorter than that of the traditional Neanderthals (it is 9.9 mm shorter than the right articular fossa of the La Ferrassie skull; Condemi (2001)). On the other hand, its width is similar to that of the left articular fossae of the La Ferrassie 1 (20.5 mm) and La Chapelle-aux-Saints (20.3 mm) skulls (Condemi, 2001).

The mastoid crest in BSV2 goes backward and upwards toward the parietal incisures, parallel to the supramastoid crest, as described by Santa Luca (1978). As described by Vallois (1969) in La Quina H27 and classical Neanderthals, the digastric groove does not join the stylomastoid foramen and shows a triangular cross-section. The mastoid notch is broad and anteriorly open, but shows a small medial bone elevation.

Applying the criteria adopted by Martinez and Arsuaga (1997) to study the temporal bone, BSV2 can be said to show a relatively flat articular eminence, a strongly projected postglenoid process, a sphenoid which does not contribute to the formation of the glenoid wall, a coronally orientated tympanic plate, a styloid process, a slightly projected mastoid process, no anterior mastoid tubercle, and a digastric groove containing a small anterior bone elevation. In view of these characteristics, the temporal bone of BSV2 corresponds more closely to those of the fossils in the "Neandertal 1" group than those of the group the latter authors called "European Middle Pleistocene" in their study (Martinez and Arsuaga, 1997).

The values of the radii of the semicircular canals in BSV2 are similar to those of the Neanderthals, especially La Chapelle-aux-Saints and La Ferrassie 2 (Spoor et al., 2003) and the Middle Pleistocene fossils. These values are similar to the mean Neanderthal values and slightly larger than the means of the Middle Pleistocene fossils obtained by Spoor et al. (2003). In comparison with the values published by Bouchneb and Crevecoeur (2009) (Table 3), BSV2 resembles the "Neanderthal lineage" means more than those of the "Middle Paleolithic modern humans".

The three-dimensional model for the left bony labyrinth of BSV2 (Fig. 8) was similar to that of the Gibraltar 1 and Petit Puymoyen 5 Neanderthals reconstructed by Spoor et al. (2003), where in particular, the posterior semicircular canal merged with the lateral canal in the superior view. Considerable pneumatisation of the petromastoid area was observed, as in the Neanderthals studied by Balzeau and Radovčić (2008).

These anatomical comparisons have some limitations, however. Like many of the fossils discovered in isotopic levels 7 to 5 and found to resemble the Neanderthals (Condemi, 2001, Mann et al., 2007), Biache-Saint-Vaast 2 is severely fragmented and poorly preserved. Geographically, this fossil is one of the most septentrional Middle Pleistocene fossils discovered so far, since most of the others were found south of the 49° northern parallel. It is therefore difficult to judge whether the characteristics differing from those of other fossils correspond to regional characteristics or sexual specificities, or result from inter-individual variability.

Except for the osseous thickening observed between the superior and inferior temporal lines on the parietal bone, the characteristics of the cranial remains of Biache-Saint-Vaast 2 mainly resemble those of the early and classical Neanderthals (Aiello and Dean, 1990; Condemi, 1988; Condemi, 1992, 2001; Dean et al., 1998; Elyaqtine, 1995; Heim, 1976; Hublin, 1988a, 1988b; Patte, 1955; Santa Luca, 1978; Spoor et al., 2003; Trinkaus, 1983, 1988), and in particular, those of Krapina 3, which is thought to be one of the early Neanderthals (Dean et al., 1998). Because of these relevant characteristics typical of early Neanderthals, it seems likely that Biache-Saint-Vaast 2 may be one of the earliest representatives of the Neanderthals discovered so far in Europe.

6. Conclusion

The Middle Pleistocene site of Biache-Saint-Vaast contained fragments of 2 human crania. The fragmented fossil Biache-Saint-Vaast 2 (frontal and nasal bone, left parietal, temporal and sphenoid bones, and the occipital bone) were studied by combining conventional morphometric methods with a virtual rebuilding technique. Although this fossil is not a complete cranium, it shows a considerable number of anatomical similarities with the early and classic Neanderthals. These characteristics are: the pattern and development of the frontal sinus; the development of the supraorbital torus; a postero-superior depression of the parietal bone corresponding to a prelambdatic depression; the alignment of the zygomatic process with the external auditory meatus; a coronally orientated tympanic plate; non alignment of the digastric groove with the base of the styloid process and the stylomastoid foramen; the pattern and dimensions of the semicircular canals. The absence of a distinct anterior mastoid tubercle, the occurrence of osseous thickening between the superior and inferior temporal lines of the parietal bone suggest that these fossils may be members of the first European Neanderthal group.

References

Aiello, L., Dean, C., 1990. An introduction to Human Evolutionary Anatomy. Academic Press, London, 596 p.

Arsuaga, J.L., Martinez, I., Gracia, A., Lorenzo, C., 1997. The Sima de los Huesos crania (Sierra de Atapuerca Spain). A comparative study. J. Hum. Evol. 33, 219–281.

Balzeau, A., Radovčić, J., 2008. Variation and modalities of growth and development of the temporal bone pneumatization in Neandertals. J. Hum. Evol. 54, 546–567.
Bouchneb, L., Crevecoeur, I., 2009. The inner ear of Nazlet Khater 2 (Upper Paleolithic Egypt). J. Hum. Evol. 56, 257–262.
Condemi, S., 1988. Caractères plésiomorphes et apomorphes de l'os temporal des néanderthaliens européens Würmiens. In: Trinkaus, E. (Ed.), L'Homme de Néandertal, 3 : l'Anatomie. ERAUL 30, Liège, pp. 49–52.
Condemi, S., 1992. Les Hommes fossiles de Saccopastore et leurs relations phylogénétiques. In: CNRS (Ed.), Paris, 174 p.
Condemi, S., 2001. Les Néandertaliens de La Chaise, Comité des travaux historiques et scientifiques. Paris, 178.
Coqueugniot, H., Le Minor, J.M., 2002. Fermeture des synchondroses intra-occipitales : implication dans la configuration du foramen magnum. C. R. Palevol 1, 35–42.
Cunningham, D.J., 1908. The evolution of the eyebrow region of the forehead with special reference to the excessive supraorbital development in the Neanderthal race. Trans. R. Soc. Edin. 46, 283–310.
Dean, D., Hublin, J.J., Holloway, R., Ziegler, R., 1998. On the phylogenetic position of the pre-Neandertal specimen from Reilingen Germany. J. Hum. Evol. 34, 485–508.
Elyaqtine, M., 1995. Variabilité et évolution de l'os temporal chez *Homo sapiens*. Comparaison avec *Homo erectus*. In: Thèse Univ. Bordeaux I, Bordeaux, 215 p.
Guipert, G., Mafart, B., Tuffreau, A., Lumley, M.A.de, 2007. 3D reconstruction and study of a new late Middle Pleistocene Hominid: Biache-Saint-Vaast 2, Nord France. Am. J. Phys. Anthropol. Suppl 44, 121–122.
Heim, J.L., 1976. Les Hommes fossiles de la Ferrassie. In: Archives de l'Institut de Paléontologie Humaine, mémoire 35. Masson Ed, Paris, 331 p.
Hublin, J.J., 1978. Quelques caractères apomorphes du crâne néandertalien et leur interprétation phylogénique. C. R. Acad. Sci. Paris, Ser. D 287, 923–926.
Hublin, J.J., 1988a. Les Présapiens Européens. In: Trinkaus, E. (Ed.), L'Homme de Néandertal, 3 : l'Anatomie. ERAUL 30, Liège, pp. 75–80.
Hublin, J.J., 1988b. Les plus anciens représentants de la lignée prénéandertalienne. In: Trinkaus, E. (Ed.), L'Homme de Néandertal, 3 : l'Anatomie. ERAUL 30, Liège, pp. 81–94.
Huxtable, J., Aikten, M.J., 1988. Datation par thermoluminescence. In: Tuffreau, A., Sommé, J. (Eds.), Le gisement paléolithique moyen de Biache-Saint-Vaast (Pas-de-Calais). Stratigraphie, environnement études archéologiques (1re partie). Mémoires de la Société Préhistorique Française, 21. t, Paris, pp. 107–108.
Lumley, M.A.de, 1973. Anténéandertaliens et Néandertaliens du bassin méditerranéen occidental européen. Éditions du Laboratoire de Paléontologie Humaine et de Préhistoire, Marseille, 626 p.
Mann, A., Vandermeersch, B., Delagnes, A., Tournepiche, J.F., 2007. Human fossil remains from the Mousterian levels of Artenac (Charente). C. R. Palevol 6, 581–589.
Martin, R., Saller, K., 1957. Lehrbuch der Anthropologie, 1/7. Gustav Fischer Verlag, Stuttgart, 661 p.
Martinez, I., Arsuaga, J.L., 1997. The temporal bones from Sima de los Huesos Middle Pleistocene site (Sierra de Atapuerca Spain). A phylogenetic approach. J. Hum. Evol. 33, 283–318.
Patte, E., 1955. Les Néanderthaliens. Masson et Cie, Paris, 560 p.
Paturet, G., 1951. Traité d'Anatomie Humaine, Ostéologie – Arthrologie – Myologie, 1. Masson et Cie, Paris, 994 p.
Rougier, H., 2003. Étude descriptive et comparative de Biache-Saint-Vaast 1 (Biache-Saint-Vaast, Pas-de-Calais, France). In: Thèse Univ. Bordeaux I, 418 p.
Santa Luca, A.P., 1978. A Re-examination of Presumed Neandertal-like Fossils. J. Hum. Evol. 7, 619–636.
Scheuer, L., Black, S., 2000. Developmental Juvenile Osteology. Elsevier Academic Press, London, 587 p.
Scheuer, L., Black, S., 2004. The Juvenile Skeleton. Elsevier Academic Press, London, 485 p.
Smith, F.H., 1976. The Neandertal Remains from Krapina: a descriptive and comparative Study, Report of investigations, n°15, Department of Anthropology. University of Tennessee, Knoxville, 359 p.
Sommé, J., Tuffreau, A., Aikten, M.J., Auguste, P., Chaline, J., Colbeaux, J.P., Cunat-Boge, N., Geeaerts, R., Hus, J., Huxtable, J., Juvigne, E., Munaut, A.V., Occhietti, S., Pichet, P., Puissegur, J.J., Rousseau, D.D., Van Vliet-Lanoe, B., 1988. Chronostratigraphie, climats et environnements. In: Tuffreau, A., Sommé, J. (Eds.), Le gisement paléolithique moyen de Biache-Saint-Vaast (Pas-de-Calais). Stratigraphie, environnement études archéologiques (1re partie). Mémoires de la Société Préhistorique Française, 21. t, Paris, pp. 115–119.
Spitery, J., 1984. L'os frontal des Hominidés fossiles. In: Thèse de Doctorat. Université de Provence, Marseille, 397 p.
Spoor, F., Zonneveld, F., 1998. A comparative review of the human bony labyrinth. Yearb. Phys. Anthropol. 41, 211–251.
Spoor, F., Wood, B., Zonneveld, F., 1994. Implications of early hominid labyrinthine morphology for evolution of human bipedal locomotion. Nature 369, 645–648.
Spoor, F., Hublin, J.J., Braun, M., Zonneveld, F., 2003. The bony labyrinth of Neanderthals. J. Hum. Evol. 44, 141–165.
Tappen, N.C., 1978. The Vermiculate Surface Pattern of Brow Ridges in Neandertal and Modern Crania. Am. J. Phys. Anthropol. 49, 1–10.
Tillier, A.M., 1977. La pneumatisation du massif cranio-facial chez les hommes actuels et fossiles. Bull. Mém Soc. Anthropol. Paris, série XIII:177–89, 287–316.
Trinkaus, E., 1973. A Reconsideration of the Fontéchevade Fossils. Am. J. Phys. Anthropol. 39, 25–36.
Trinkaus, E., 1983. The Shanidar Neanderthals. Academic Press, New York, 502 p.
Trinkaus, E., 1988. The evolutionary origins of the Neandertals, or why were there Neandertals? In: Trinkaus, E. (Ed.), L'Homme de Néandertal, 3 : l'Anatomie. ERAUL 30, Liège, pp. 11–29.
Tuffreau, A., 1988a. Historique des fouilles à Biache-Saint-Vaast. In: Tuffreau, A., Sommé, J. (Eds.), Le gisement paléolithique moyen de Biache-Saint-Vaast (Pas-de-Calais). Stratigraphie, environnement études archéologiques (1re partie). Mémoires de la Société Préhistorique Française, 21. t, Paris, pp. 15–24.
Tuffreau, A., 1988b. Stratigraphie de la séquence archéologique. In: Tuffreau, A., Sommé, J. (Eds.), Le gisement paléolithique moyen de Biache-Saint-Vaast (Pas-de-Calais). Stratigraphie, environnement études archéologiques (1re partie). Mémoires de la Société Préhistorique Française, 21. t, Paris, pp. 123–131.
Tuffreau, A., Munaut, V., Puissegur, J.-J., Sommé, J., 1982. Stratigraphie et environnement de la séquence archéologique de Biache-Saint-Vaast (Pas-de-Calais). Bull. A. F. E. Q. 10-11, 57–61.
Vallois, H.V., 1969. Le temporal néandertalien H 27 de la Quina. Étude anthropologique. L'Anthropologie Paris 73:365–400, 525–544.
Vandermeersch, B., 1978. Étude préliminaire du crâne humain du gisement paléolithique de Biache-Saint-Vaast (Pas-de-Calais). Bull. A. F. E. Q. 54-55-56, 65–67.
Vandermeersch, B., 1982. L'Homme de Biache-Saint-Vaast. Comparaison avec l'Homme de Tautavel. In: CNRS (Ed.), 1er Congrès international de Paléontologie Humaine. L'*Homo erectus* et la place de l'Homme de Tautavel parmi les Hominidés Fossiles. Nice, pp. 894–900.
Vlček, E., 1967. Die Sinus Frontales bei europäischen Neandertalern. Anthrop. Anz. 30, 166–189.
Yokoyama, Y., 1989. Direct gamma-ray spectrometric dating of Anteneandertalian and Neandertalian remains. In: Giacobini, G. (Ed.), *Hominidae*, Proceedings of the 2nd intern. Congress of Human Paleontology, Turin, pp. 387–390.